



Research Article

A study on numerical solutions of a fractional-order model for CAR T-cell therapy in leukemia using the laplace-adomian decomposition method

Rezaul KARİM^{1,2,*}, M. Ali AKBAR², M. A. BKAR PK², Pinakee DEY¹

¹Department of Mathematics, Mawlana Bhashani Science and Technology University, 1902, Bangladesh

²Department of Applied Mathematics, University of Rajshahi, 6205, Bangladesh

ARTICLE INFO

Article history

Received: 25 October 2024

Revised: 13 January 2025

Accepted: 13 February 2025

Keywords:

CAR T-cell; Fractional Order (FO); Mathematical Model (MM); Leukemia Disease; Stability Analysis

ABSTRACT

Leukemia is an aggressive form of blood cancer that develops in the bone marrow. In this study, we consider a fractional-order four compartmental mathematical model of leukemia which includes susceptible blood cells $S(t)$, infected blood cells $I(t)$, cancer cells $C(t)$, and immune blood cells $W(t)$, and we discuss the dynamics of transmission of the disease. We employ the Laplace-Adomian decomposition methods to obtain analytical solutions and the Runge-Kutta fourth-order approach to get numerical solutions for the mathematical model of leukemia. In order to illustrate the process, the convergent of the series solution is also given, and the corresponding plots against various orders of the differentiations are plotted using specific values for the model's parameters. We compared the solutions determined from the Laplace-Adomian decomposition methods and Runge-Kutta fourth-order. Graphical results demonstrate that the Laplace Adomian Decomposition method aligns closely with the Runge-Kutta fourth order method. For various fractional parameter values α the findings reveal that the fractional-order model offers more accuracy and stability compared to the conventional integer-order model. Some plots are presented to show the reliability and simplicity of the method. Leukemia virus is one of the many infectious diseases whose dynamics of spread can be better understood through mathematical modeling and underscores the urgent need to ensure global accessibility to this approach, with the potential to save countless lives worldwide.

Cite this article as: Karim R, Akbar MA, Bkar PK MA, Dey P. A study on numerical solutions of a fractional-order model for CAR T-cell therapy in leukemia using the laplace-adomian decomposition method. Sigma J Eng Nat Sci 2026;44(2):954–969.

INTRODUCTION

Leukemia originates from a cell in the bone marrow that undergoes a transformation into a leukemia cell. After this change, the leukemia cells may start to grow and

thrive more effectively than healthy cells. Gradually, these leukemia cells can outnumber or inhibit the production of normal cells. Between 2009 and 2014, leukemia stayed the 5th leading cause of cancer passing away in males and the

*Corresponding author.

*E-mail address: rezaulmath11124@gmail.com

This paper was recommended for publication in revised form by Editor-in-Chief Ahmet Selim Dalkilic



6th in females. By 2016, around 2.35 million people worldwide be situated living with leukemia, leading to about 353,500 passing away [1-2]. Scientific biological problems are modeled using the fascinating field of applied analysis known as fractional calculus, which is made up of free-order derivatives and integrals. A tumor is an uncontrolled growth of abnormal cells that can invade tissues. This treatment is altering the immune system and allows them to specifically target and destroy leukemia cells [3-4]. Numerous researchers have also reviewed studies using CAR-T in the leukemia model [5-6]. By delivering CAR T- cells, [7] examined the MM of the interaction between leukemia cells and immune cells. Our funding has been allocated to a broad range of cancer types, which are classified according to the predominant cell type impacted [8]. As numerous studies have shown [3,9-11], FO modeling is becoming more and more popular in the field of epidemiology because it can accurately represent intricate and nonlinear disease processes. The Atangana-Baleanu and Caputo-Fabrizio models are two well-known instances of fractional-order models that shed light on the dynamics of disease and the impact of healthcare capacity on disease transmission. As mentioned in references [12-15]. It presents the multistep LADM, which provides a more accurate approximation than conventional methods for modeling the dynamics of T-cells [16-19]. It discusses convergence and error while building method spaces and using Caputo's partial time derivative [20-22]. Maayah et al. explored approximate results and symmetrical attractors for an FO cancer-immune model using the method in [23,24]. Additionally, studies have investigated an in-host dengue contagion model with invulnerable comeback and proposed an innovative algorithm that integrates cubic uniform splines with limited difference techniques to solve FO diffusion singular wave models affected by damping-reaction forces [25-28]. Ponalagusamy et al. [29] explored the approximate solution of heat flow problems using a hybrid approach that combines the Rayleigh-Ritz method with STWS and RKHM techniques. In a separate study, Ponalagusamy [30] developed an inventive and effective computational procedure founded on STWS for comprehensive linear time-varying structures, including both singular and non-singular cases. Ponalagusamy and Senthilkumar [31] conducted a comparative analysis of various Runge-Kutta (RK4) orders and embedded methods in the simulation of multilayer raster CNNs. Additionally, Ponalagusamy et al. [32] introduced a new 5th-order, 5th-stage RK4 method based on the Heronian mean. Chandru et al. [33] proposed a 5th weighted Runge-Kutta algorithm, also derived using the Heronian mean, for solving initial value problems in ordinary differential equations. Furthermore, Ponalagusamy and Senthilkumar [34] developed a fourth-order embedded RK algorithm with Heronian mean incorporating error control for single-layer or raster cellular neural networks. Atalan et al. [35] developed optimization models to assess and

improve the performance of healthcare systems. Dincer [36] analyzed mathematical modeling to determine the nickel inhibition constant in nitrification processes. Berrak and Ali [37] examined the stability of a neural field model incorporating small delays. Results are shown for convergence-error behavior and computational algorithms. A summary and suggestions for more research are included in the study's conclusion, which investigates the use of fractional differential equations in the modeling of diseases such as cancer and infectious diseases, with a particular emphasis on the relationship between cancer cells and the immune system. Important topics like the mathematical framework, error analysis, and solution representation are covered. Summaries of the findings and recommendations for further study are provided at the end. The work closes research gaps concerning the T-cells model by using a novel FO modeling system to realize how the virus spreads within a mass with adaptive invulnerability. The numerical solutions of the given FO model are analyzed using the ADM in combination with the Laplace transform. To validate the results, random values are assigned to the initial conditions and parameters. In this study, we develop and analyze a mathematical model (MM) for leukemia, represented by a system of FO differential equations. The model consists of four compartmental components: Fractional order $S(t)$, $I(t)$, $C(t)$, and $W(t)$ [38-39]. We aim to investigate the numerical simulations, graphical representations, parameter analyses, interpretations, and solutions of the fractional-order model using the RK4 method and the LADM. The results obtained from LADM are compared with those derived from numerical simulations. We present solution figures generated through LADM and simulate them alongside the numerical solutions for comparison. This analysis highlights the accuracy, simplicity, and effectiveness of the LADM approach. By including FO derivatives, the model can more exactly enlighten derivatives that are common in biological organizations but are often missed in conventional integer-order models, and many researchers have described [40-45].

This work is systematized as follows: Section 2 covers the preliminaries, providing foundational concepts. Section 3 offers a detailed description of the mathematical model (compartmental structure) for leukemia. Section 4 outlines the solution steps using the LADM method. Section 5 delves into the analysis of the fractional model, while Section 6 examines the solutions in detail. The Numerical simulations are presented in Section 7, which includes a subsection (7.1) focused on numerical simulations and result comparisons. Section 8 explores the stability criteria for the FO leukemia model, and Section 9 discusses the convergence analysis for the model. Lastly, Section 10 concludes the study and highlights possible directions for future research.

PRELIMINARIES

The Reimann-Liouville fractional (RLF) θ -order integral operator, where the function $q : R_+ \rightarrow R$, expressed $J^\theta q(t)$ is expressed as

$$J^\theta q(t) = \frac{1}{\Gamma(\theta)} \int_0^t \frac{q(\xi)}{(t-\xi)^{1-\theta}} d\xi.$$

Where $\theta \in R_+ : \theta \in (0,1)$ and $t > 0$. The gamma function $\Gamma(\theta)$ is given by

$$\Gamma(\theta) = \int_0^\infty x^{\theta-1} e^{-x} dx$$

Mathematical Model (Compartment) of Leukemia

By integrating experimental data and theoretical analysis, the model can guide clinical practice and contribute to improving patient outcomes in cancer immune treatment. We will use a system of ODEs to describe the dynamics of (CAR) T Cell Treatment. Here $S(t)$ represents the number of susceptible blood cell class, $I(t)$ represent the number of infected blood cell class, $C(t)$ represent the number of leukemia cell class and $W(t)$ represent the number of immune blood cells. Here, Figure 1 represents the leukemia transmission with a compartment model. According to Khumaeroh et al. [4], Khatun and Biswas [8] model, we considered as:

The natural mortality rates of $S(t)$, $I(t)$, $C(t)$, and $W(t)$ are represented by the parameters α , μ , b , and τ , respectively. Due to the presence of $C(t)$ in the blood, the decay rate of $W(t)$ is indicated by the letter θ , ν is the rate at which T cells and the proliferation rate of $W(t)$ is δ . Here, Figure 1 represents the Leukaemia transmission with the compartment model. The following set of ordinary differential equations governs our modified model Khumaeroh et al. [4], Khatun and Biswas [8] and karim et al. [36] is as:

$$\left. \begin{aligned} \frac{dS}{dt} &= A - \alpha S - \beta SC, \\ \frac{dI}{dt} &= \beta SC - \mu I - \gamma CI, \\ \frac{dC}{dt} &= r(1 - bC)C - kCW, \\ \frac{dW}{dt} &= \nu + \delta C - \tau W - \theta WC. \end{aligned} \right\} \quad (1)$$

and $S(t) \geq 0, I(t) \geq 0, C(t) \geq 0$ and $W(t) \geq 0$. (2)

Steps of Solutions of LADM

The ADM, introduced by Adomian in 1980, is a robust approach for obtaining numerical and explicit solutions to systems of DEs arising in physical problems. The LT, widely recognized as a powerful tool in manufacturing and applied mathematics, complements ADM effectively. The integration of these two methods gives rise to the LADM, a highly efficient technique. In LADM, the LT is applied to convert DEs into algebraic equations, while nonlinear terms are expressed in terms of Adomian polynomials. This method is well-suited for solving deterministic and stochastic differential equations, including systems of linear and nonlinear ordinary and partial differential equations of both classical and fractional orders. Unlike other methods, LADM does not require perturbation, linearization, or a predefined step size, as in the RK4. Additionally, it does not depend on parameters like the Homotopy Perturbation Method (HPM). Although the solutions obtained through LADM align with those derived from the standard ADM, LADM is considered more powerful.

Let us consider the following FO differential equation given by

$$c_{j\infty} V(t) = L_i(V_1, V_2, V_3 \dots \dots V_i) + Z_i(V_1, V_2, V_3 \dots \dots V_i). Y$$

Subject to

$$V^\alpha(0) = C_k^i, \text{ for } i = 1, 2, 3, \dots \dots m, \text{ and } n_{i-1} \leq \alpha \leq n_i.$$

Where $c_{j\infty} V_i(t)$ is Caputo–Fabrizio operator of i number of unspecified functions $P(t)$.

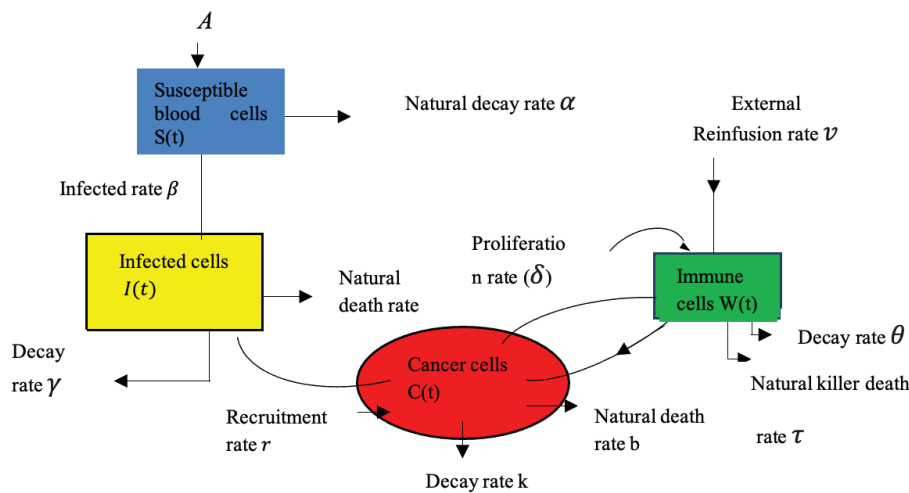


Figure 1. Leukaemia transmission with a compartment model.

Now from Equation (2), on (1) yields:

$$\frac{sL[V_i(t)] - V_i(0)}{s+\alpha(1-s)} = L[L_i(V_1, V_2, V_3, \dots, V_i) + Z_i(V_1, V_2, V_3, \dots, V_i)].$$

Utilizing the ADM, the unknown function is decomposed as:

$$V_i(t) = \sum_{j=0}^{\infty} V_{ij}(t), \quad i = 1, 2, 3, \dots, m.$$

Where, $Z_i(w_1, \dots, w_i) = \sum_{j=0}^{\infty} X_{ij}(t), i = 1, 2, 3, \dots, m.$ and A_{ij} is the using the definition of an adomian polynomial, one obtains:

$$L[\sum_{j=0}^{\infty} V_{ij}(t)] = \frac{V_i^{ki}(0)}{s} + \frac{s+\alpha(1-s)}{s} (L[L_i(\sum_{j=0}^{\infty} V_{1j}(t), \dots, \sum_{j=0}^{\infty} V_{mj}(t))] + L[\sum_{j=0}^{\infty} X_{ij}(t)]).$$

Now from equation (4), $w_{1j}, w_{2j}, \dots, w_{mj}, j \geq 0$:

$$V_{i(j+1)}(t) = L^{-1} \left(\frac{V_i^{ki}(0)}{s} \right) + L^{-1} \left(\frac{s + \alpha(1-s)}{s} L \times \left[L_i \left(\sum_{j=0}^{\infty} V_{1j}(t), \dots, \sum_{j=0}^{\infty} V_{mj}(t) \right) \right] + L \left[\sum_{j=0}^{\infty} X_{ij}(t) \right] \right)$$

which simplifies to the equations be

$$V_{i(j+1)}(t) = C_k^i + L^{-1} \left(\frac{s+\alpha(1-s)}{s} L \left[L_i \left(\sum_{j=0}^{\infty} V_{1j}(t), \dots, \sum_{j=0}^{\infty} V_{mj}(t) \right) \right] + L \left[\sum_{j=0}^{\infty} X_{ij}(t) \right] \right)$$

Applying FO and Caputo-derivative methods, we have

$$\left. \begin{aligned} \frac{{}^c d^\alpha S(t)}{dt} &= A - \alpha S - \beta SC, \\ \frac{{}^c d^\alpha I(t)}{dt} &= \beta SC - \mu I - \gamma CI, \\ \frac{{}^c d^\alpha C(t)}{dt} &= r(1 - bC)C - kW, \\ \frac{{}^c d^\alpha W(t)}{dt} &= v + \delta C - \tau M - \theta WC. \end{aligned} \right\} \quad (3)$$

where $\mu = \mu_1 + \frac{\eta\beta}{\delta}$ and $\delta = \delta_1 + \frac{\eta}{\delta\theta}$

If the equations (3) be $\frac{{}^c d^\alpha S(t)}{dt} \geq 0, \frac{{}^c d^\alpha I(t)}{dt} \geq 0, \frac{{}^c d^\alpha C(t)}{dt} \geq 0$ and $\frac{{}^c d^\alpha W(t)}{dt} \geq 0$ respectively. Now from Equations (3) we get,

$$\left. \begin{aligned} C_{j\alpha 1} S(t) &= A - \alpha S(t) - \beta S(t)C(t), \\ C_{j\alpha 1} I(t) &= \beta S(t)C(t) - \mu I(t) - \gamma C(t)I(t), \\ C_{j\alpha 1} C(t) &= r(1 - bC(t))C(t) - kC(t)W(t), \\ C_{j\alpha 1} W(t) &= v + \delta C(t) - \tau W(t) - \theta W(t)C(t). \end{aligned} \right\} \quad (4)$$

With initial conditions

$$S(0) = S_0, I(0) = I_0, C(0) = C_0, W(0) = W_0 \quad (5)$$

On the provided fractional-order model, numerical solutions are examined by utilizing the (ADM) in conjunction with the LT. Both the initial conditions and parameter values are randomly assigned in order to validate the generated results.

Variables and Parameter Analysis of the Fractional Order Model

Table 1-2 in this section presents the definitions of each compartment along with detailed descriptions of the parameters used in the model (Altrock et al. [2], Khumaeroh et al. [4], and Khatun and Biswas [8]).

Table 1. Variables and parameter description of the fractional order leukemia model

Variables / parameters	Descriptions	Area	Unit
S	Susceptible blood cell class	$S \geq 0$	Concentration
I	Infected class	$I \geq 0$	Concentration
C	Leukemia blood cell class	$C \geq 0$	Concentration
W	Immune blood cell class	$W \geq 0$	Concentration
A	Recruitment rate of susceptible blood cells	$A \geq 0$	Concentration/day
μ	Natural death rate	$\mu \geq 0$	Concentration/day
α	Changing rate of susceptible class to infected class	$\alpha \geq 0$	1/day
γ	Infected cells natural death rate	$\gamma \geq 0$	Concentration/day
β	Decay rate of Infected cells	$\beta \geq 0$	Concentration/day
r	Progress rate of Leukemia blood cell	$r \geq 0$	1/day
θ	Carrying capacity of Leukemia blood cell	$\theta \geq 0$	Concentration/day
ν	Exterior distillation rate of T-Cell Treatment	$\nu \geq 0$	Concentration/day
τ	Natural death rate of Recovered cell	$\tau \geq 0$	1/day
δ	Immune cell of proliferation rate	$\delta > 0$	1/day

Table 2. Purpose of the specific parameter of MM of leukemia (Khumaeroh et al. [4], Khatun and Biswas [8] and Karim et al. [36]).

Parameter	Cancer: endemic balance prior to intervention	After treatment, the endemic equilibrium is free of cancer	The cancer endemic equilibrium following treatment
A	1	1	1
α	0.001	0.01	0.001
β	0.00005	0.00001	0.00005
μ	0.0002	0.003	0.0002
γ	0.001	0.001	0.001
δ	0.01	0.03	0.01
r	0.18	0.019	0.18
b	0.001	0.001	0.001
k	0.005	0.04	0.005
ν	0	0.5	1
τ	0.001	0.006	0.05
θ	0.002	0.01	0.002

Solutions

Taking the LT on both sides in Eq. (3), we attain the succeeding:

$$\left. \begin{aligned} L\{C_{j\theta}S(t)\} &= L\{A - \alpha S(t) - \beta S(t)C(t)\}, \\ L\{C_{j\theta}I(t)\} &= L\{\beta S(t)C(t) - \mu I(t) - \gamma C(t)I(t)\}, \\ L\{C_{j\theta}C(t)\} &= L\{r(1 - bC(t))C(t) - kC(t)W(t)\}, \\ L\{C_{j\theta}W(t)\} &= L\{\nu + \delta C(t) - \tau W(t) - \theta W(t)C(t)\}. \end{aligned} \right\} \quad (6)$$

$$\left. \begin{aligned} S^\theta S(t) - S^{\theta-1}S(0) &= L\{A - \alpha S(t) - \beta S(t)C(t)\}, \\ S^\theta C(t) - S^{\theta-1}C(0) &= L\{r(1 - bC(t))C(t) - kC(t)W(t)\}, \\ S^\theta I(t) - S^{\theta-1}I(0) &= L\{\beta S(t)C(t) - \mu I(t) - \gamma C(t)I(t)\}, \\ S^\theta W(t) - S^{\theta-1}W(0) &= L\{\nu + \delta C(t) - \tau W(t) - \theta W(t)C(t)\}. \end{aligned} \right\} \quad (7)$$

$$\left. \begin{aligned} S^\theta S(t) &= S^{\theta-1}S(0) + L\{A - \alpha S(t) - \beta S(t)C(t)\}, \\ S^\theta C(t) &= S^{\theta-1}C(0) + L\{r(1 - bC(t))C(t) - kC(t)W(t)\}, \\ S^\theta I(t) &= S^{\theta-1}I(0) + L\{\beta S(t)C(t) - \mu I(t) - \gamma C(t)I(t)\}, \\ S^\theta W(t) &= S^{\theta-1}W(0) + L\{\nu + \delta C(t) - \tau W(t) - \theta W(t)C(t)\}. \end{aligned} \right\} \quad (8)$$

$$\left. \begin{aligned} S(t) &= S^{-1}S(0) + \frac{1}{s^\theta} L\{A - \alpha S(t) - \beta S(t)C(t)\}, \\ I(t) &= S^{-1}I(0) + \frac{1}{s^\theta} L\{\beta S(t)C(t) - \mu I(t) - \gamma C(t)I(t)\}, \\ C(t) &= S^{-1}C(0) + \frac{1}{s^\theta} L\{r(1 - bC(t))C(t) - kC(t)W(t)\}, \\ W(t) &= S^{-1}W(0) + \frac{1}{s^\theta} L\{\nu + \delta C(t) - \tau W(t) - \theta W(t)C(t)\}. \end{aligned} \right\} \quad (9)$$

Assuming that the solution $S(t), I(t), C(t), W(t)$ are in form infinite series by

$$\begin{aligned} S(t) &= \sum_{n=0}^{\infty} S_n, I(t) = \sum_{n=0}^{\infty} I_n, \\ C(t) &= \sum_{n=0}^{\infty} C_n, W(t) = \sum_{n=0}^{\infty} W_n, \end{aligned} \quad (10)$$

and non-linear term involved in the model are $S(t), I(t), C(t), W(t)$ are decomposed by Adomaim.

$$S(t)C(t) = \sum_{n=0}^{\infty} A_n, C(t)I(t) = \sum_{n=0}^{\infty} B_n, W(t)C(t) = \sum_{n=0}^{\infty} D_n$$

where A_n, B_n and C_n are Adomain polynomial given by

$$\begin{aligned} A_n &= \frac{1}{\Gamma(n+1)} \frac{d^n}{dt^n} \left[\sum_{k=0}^n \lambda^k S_k \sum_{k=0}^n \lambda^n C_k \right] \lambda, \\ B_n &= \frac{1}{\Gamma(n+1)} \frac{d^n}{dt^n} \left[\sum_{k=0}^n \lambda^k C_k \sum_{k=0}^n \lambda^n I_k \right] \lambda, \\ D_n &= \frac{1}{\Gamma(n+1)} \frac{d^n}{dt^n} \left[\sum_{k=0}^n \lambda^k W_k \sum_{k=0}^n \lambda^n C_k \right] \lambda. \end{aligned} \quad (12)$$

Substitute Equation (10)-(12) in the Eq. (9) we get,

$$\begin{aligned} S(t) &= S^{-1}S(0) + \frac{1}{s^\theta} L\{A - \alpha S_n(t) - \beta A_n\}, \\ I(t) &= S^{-1}I(0) + \frac{1}{s^\theta} L\{\beta A_n - \mu I_n(t) - \gamma B_n\}, \\ C(t) &= S^{-1}C(0) + \frac{1}{s^\theta} L\{r(1 - bC_n(t))C_n(t) - kD_n\}, \\ W(t) &= S^{-1}W(0) + \frac{1}{s^\theta} L\{\nu + \delta C_n(t) - \tau W_n(t) - \theta D_n\}. \end{aligned} \quad (13)$$

Using initial condition in Equation (13) we have,

$$\begin{aligned} S(t) &= \frac{n_1}{s} + \frac{1}{s^\theta} L\{A - \alpha S_n(t) - \beta A_n\} \\ I(t) &= \frac{n_2}{s} + \frac{1}{s^\theta} L\{\beta A_n - \mu I_n(t) - \gamma B_n\} \\ C(t) &= \frac{n_3}{s} + \frac{1}{s^\theta} L\{r(1 - bC_n(t))C_n(t) - kD_n\} \\ W(t) &= \frac{n_4}{s} + \frac{1}{s^\theta} L\{\nu + \delta C_n(t) - \tau W_n(t) - \theta D_n\} \end{aligned} \quad (14)$$

We iterate term in Eq (14) we get,

$$\begin{aligned} \sum_{n=0}^{\infty} S_{(n+1)}(t) &= L^{-1} \left[\frac{1}{S^\theta} L\{A - \alpha S_n(t) - \beta A_n\} \right], \\ \sum_{n=0}^{\infty} I_{(n+1)}(t) &= L^{-1} \left[\frac{1}{S^\theta} L\{\beta A_n - \mu I_n(t) - \gamma B_n\} \right], \\ \sum_{n=0}^{\infty} C_{(n+1)}(t) &= L^{-1} \left[\frac{1}{S^\theta} L[\{r(1 - bC_n(t))C_n(t) - kD_n\}] \right] \\ \sum_{n=0}^{\infty} W_{(n+1)}(t) &= L^{-1} \left[\frac{1}{S^\theta} L\{v + \delta C_n(t) - \tau W_n(t) - \theta D_n\} \right] \end{aligned} \tag{15}$$

The followings were obtained from equation (15) we get,

$$S_{(0)} = n_1, I_{(0)} = n_2, C_{(0)} = n_3, W_{(0)} = n_4 \tag{16}$$

When $n = 0$, from first Eq. of (15)

$$\begin{aligned} S_1 &= L^{-1} \left[\frac{1}{S^\theta} L\{A - \alpha S_0(t) - \beta A_0\} \right], \\ &= L^{-1} \left[\frac{1}{S^\theta} L\{A - \alpha n_1 - \beta n_1 n_3\} \right], \\ &= L^{-1} \left[\frac{1}{S^\theta} * \frac{1}{S} \{A - \alpha n_1 - \beta n_1 n_3\} \right], \\ &= L^{-1} \left[\{A - \alpha n_1 - \beta n_1 n_3\} \frac{1}{S^{\theta+1}} \right], \\ S_1 &= \{A - \alpha n_1 - \beta n_1 n_3\} \frac{t^\theta}{\Gamma(\theta+1)} \end{aligned} \tag{17}$$

When $n = 0$ in second Eq. of (15) we get,

$$\begin{aligned} I_1 &= L^{-1} \left[\frac{1}{S^\theta} L\{\beta A_n - \mu I_n(t) - \gamma B_n\} \right], \\ &= L^{-1} \left[\frac{1}{S^\theta} L\{\beta n_1 n_3 - \mu n_3 - \gamma n_2 n_3\} \right], \\ &= L^{-1} \left[\frac{1}{S^\theta} * \frac{1}{S} \{\beta n_1 n_3 - \mu n_3 - \gamma n_2 n_3\} \right], \\ &= L^{-1} \left[\{\beta n_1 n_3 - \mu n_3 - \gamma n_2 n_3\} \frac{1}{S^{\theta+1}} \right], \\ I_1 &= (\beta n_1 n_3 - \mu n_3 - \gamma n_2 n_3) \frac{t^\theta}{\Gamma(\theta+1)} \end{aligned} \tag{18}$$

Also, when $n = 0$ in third Eq. of (15), we get

$$\begin{aligned} C_1 &= L^{-1} \left[\frac{1}{S^\theta} L[\{r(1 - bC_n(t))C_n(t) - kD_n\}] \right] \\ &= L^{-1} \left[\frac{1}{S^\theta} L\{r(1 - bn_3)n_3 - kn_3n_4\} \right] \\ &= L^{-1} \left[\frac{1}{S^\theta} * \frac{1}{S} \{r(1 - bn_3)n_3 - kn_3n_4\} \right] \\ &= L^{-1} \left[\{r(1 - bn_3)n_3 - kn_3n_4\} \frac{1}{S^{\theta+1}} \right] \\ C_1 &= \{r(1 - bn_3)n_3 - kn_3n_4\} \frac{t^\theta}{\Gamma(\theta+1)} \end{aligned} \tag{19}$$

Again when $n = 0$ in 4th Eq. of (15)

$$\begin{aligned} W_1 &= L^{-1} \left[\frac{1}{S^\theta} L\{v + \delta C_0(t) - \tau W_0(t) - \theta D_0\} \right] \\ &= L^{-1} \left[\frac{1}{S^\theta} L\{v + \delta n_3 - \tau n_4 - \theta n_3 n_4\} \right] \\ &= L^{-1} \left[\frac{1}{S^\theta} * \frac{1}{S} \{v + \delta n_3 - \tau n_4 - \theta n_3 n_4\} \right] \\ &= L^{-1} \left[\{v + \delta n_3 - \tau n_4 - \theta n_3 n_4\} \frac{1}{S^{\theta+1}} \right] \\ W_1 &= \{v + \delta n_3 - \tau n_4 - \theta n_3 n_4\} \frac{t^\theta}{\Gamma(\theta+1)} \end{aligned} \tag{20}$$

Similarly, when $n = 1$ then equation (10) in first

Equation we get

$$\begin{aligned} S_2 &= L^{-1} \left[\frac{1}{S^\theta} L\{A - \alpha S_1(t) - \beta A_1\} \right] \\ &= L^{-1} \left[\frac{1}{S^\theta} L \left\{ A - \alpha(A - \alpha n_1 - \beta n_1 n_3) \frac{t^\theta}{\Gamma(\theta+1)} \right. \right. \\ &\quad \left. \left. - \beta \left(n_3(A - \alpha n_1 - \beta n_1 n_3) \frac{t^\theta}{\Gamma(\theta+1)} + n_1 \{r(1 - bn_3)n_3 - kn_3n_4\} \frac{t^\theta}{\Gamma(\theta+1)} \right) \right\} \right] \\ &= L^{-1} \left[\frac{1}{S^\theta} * \left\{ A - \alpha(A - \alpha n_1 - \beta n_1 n_3) \frac{\Gamma(\theta+1)}{\Gamma(\theta+1)S^{\theta+1}} \right. \right. \\ &\quad \left. \left. - \beta \left(n_3(A - \alpha n_1 - \beta n_1 n_3) \frac{\Gamma(\theta+1)}{\Gamma(\theta+1)S^{\theta+1}} + n_1 \{r(1 - bn_3)n_3 - kn_3n_4\} \frac{\Gamma(\theta+1)}{\Gamma(\theta+1)S^{\theta+1}} \right) \right\} \right] \\ &= L^{-1} \left[\frac{1}{S^\theta} * \left\{ A - \alpha(A - \alpha n_1 - \beta n_1 n_3) \frac{1}{S^{\theta+1}} \right. \right. \\ &\quad \left. \left. - \beta \left(n_3(A - \alpha n_1 - \beta n_1 n_3) \frac{1}{S^{\theta+1}} + n_1 \{r(1 - bn_3)n_3 - kn_3n_4\} \frac{1}{S^{\theta+1}} \right) \right\} \right] \\ &= L^{-1} \left[\left\{ A - \alpha(A - \alpha n_1 - \beta n_1 n_3) \frac{1}{S^{2\theta+1}} \right. \right. \\ &\quad \left. \left. - \beta \left(n_3(A - \alpha n_1 - \beta n_1 n_3) \frac{1}{S^{2\theta+1}} + n_1 \{r(1 - bn_3)n_3 - kn_3n_4\} \frac{1}{S^{2\theta+1}} \right) \right\} \right] \\ S_2 &= L^{-1} \left[\left\{ A - \alpha(A - \alpha n_1 - \beta n_1 n_3) \frac{t^{2\theta}}{\Gamma(2\theta+1)} - \beta \left(n_3(A - \alpha n_1 - \beta n_1 n_3) \frac{t^{2\theta}}{\Gamma(2\theta+1)} + n_1 \{r(1 - bn_3)n_3 - kn_3n_4\} \frac{t^{2\theta}}{\Gamma(2\theta+1)} \right) \right\} \right] \end{aligned} \tag{21}$$

Similarly, when $n = 1$ then equation (15) in 2nd equation

we get

$$\begin{aligned}
 &= L^{-1} \left[\left\{ r \left(1 - b \{ r(1 - bn_3)n_3 - kn_3n_4 \} \frac{1}{S^{2\theta+1}} \right. \right. \right. \\
 &\quad \left. \left. * \{ r(1 - bn_3)n_3 - kn_3n_4 \} \frac{1}{S^{2\theta+1}} \right) - kn_4 \{ r(1 - bn_3)n_3 \right. \right. \\
 &\quad \left. \left. - kn_3n_4 \right\} \frac{1}{S^{2\theta+1}} + n_3 \{ (v + \delta n_3 - \tau n_4 \right. \right. \\
 &\quad \left. \left. - \theta n_3n_4 \} \frac{1}{S^{2\theta+1}} \right\} \right] \\
 &= L^{-1} \left[\left\{ r \left(1 - b \{ r(1 - bn_3)n_3 - kn_3n_4 \} \frac{t^{2\theta}}{\Gamma(2\theta+1)} \right. \right. \right. \\
 &\quad \left. \left. * \{ r(1 - bn_3)n_3 - kn_3n_4 \} \frac{t^{2\theta}}{\Gamma(2\theta+1)} \right) \right. \right. \\
 &\quad \left. \left. - kn_4 \{ r(1 - bn_3)n_3 - kn_3n_4 \} \frac{t^{2\theta}}{\Gamma(2\theta+1)} \right. \right. \\
 &\quad \left. \left. + n_3 \{ (v + \delta n_3 - \tau n_4 - \theta n_3n_4) \frac{t^{2\theta}}{\Gamma(2\theta+1)} \} \right\} \right] \quad (23)
 \end{aligned}$$

Similarly, when $n = 1$ then equation (15) in fourth Equation we get

$$\begin{aligned}
 W_2 &= L^{-1} \left[\frac{1}{S^\theta} * L \{ v + \delta C_1(t) - \tau W_1(t) - \theta D_1 \} \right] \\
 W_2 &= L^{-1} \left[\frac{1}{S^\theta} * L \left\{ v + \delta (b \{ r(1 - bn_3)n_3 \right. \right. \right. \\
 &\quad \left. \left. - kn_3n_4 \} \frac{t^\theta}{\Gamma(\theta+1)}) - \tau \{ v + \delta n_3 - \tau n_4 \right. \right. \\
 &\quad \left. \left. - \theta n_3n_4 \} \frac{t^\theta}{\Gamma(\theta+1)} - \theta n_4 \{ r(1 - bn_3)n_3 \right. \right. \\
 &\quad \left. \left. - kn_3n_4 \} \frac{t^\theta}{\Gamma(\theta+1)} + n_3 \{ (v + \delta n_3 - \tau n_4 \right. \right. \\
 &\quad \left. \left. - \theta n_3n_4 \} \frac{t^\theta}{\Gamma(\theta+1)}) \right\} \right] \\
 &= L^{-1} \left[\frac{1}{S^\theta} * \left\{ v + \delta (b \{ r(1 - bn_3)n_3 \right. \right. \right. \\
 &\quad \left. \left. - kn_3n_4 \} \frac{\Gamma(\theta + 1)}{\Gamma(\theta + 1)S^{\theta+1}} \right) \right. \right. \\
 &\quad \left. \left. - \tau \{ v + \delta n_3 - \tau n_4 - \theta n_3n_4 \} \frac{\Gamma(\theta + 1)}{\Gamma(\theta + 1)S^{\theta+1}} \right. \right. \\
 &\quad \left. \left. - \theta n_4 \{ r(1 - bn_3)n_3 - kn_3n_4 \} \frac{\Gamma(\theta + 1)}{\Gamma(\theta + 1)S^{\theta+1}} \right. \right. \\
 &\quad \left. \left. + n_3 \{ (v + \delta n_3 - \tau n_4 - \theta n_3n_4) \frac{\Gamma(\theta + 1)}{\Gamma(\theta + 1)S^{\theta+1}} \} \right\} \right] \\
 &= L^{-1} \left[\frac{1}{S^\theta} * \left\{ v + \delta (b \{ r(1 - bn_3)n_3 - kn_3n_4 \} \frac{1}{S^{\theta+1}} \right. \right. \right. \\
 &\quad \left. \left. - \tau \{ v + \delta n_3 - \tau n_4 - \theta n_3n_4 \} \frac{1}{S^{\theta+1}} \right. \right. \\
 &\quad \left. \left. - \theta n_4 \{ r(1 - bn_3)n_3 - kn_3n_4 \} \frac{1}{S^{\theta+1}} \right. \right. \\
 &\quad \left. \left. + n_3 \{ (v + \delta n_3 - \tau n_4 - \theta n_3n_4) \frac{1}{S^{\theta+1}} \} \right\} \right]
 \end{aligned}$$

$$\begin{aligned}
 &= L^{-1} \left[\left\{ v + \delta (b \{ r(1 - bn_3)n_3 - kn_3n_4 \} \frac{1}{S^{2\theta+1}} \right) \right. \right. \\
 &\quad \left. \left. - \tau \{ v + \delta n_3 - \tau n_4 - \theta n_3n_4 \} \frac{1}{S^{2\theta+1}} \right. \right. \\
 &\quad \left. \left. - \theta n_4 \{ r(1 - bn_3)n_3 - kn_3n_4 \} \frac{1}{S^{2\theta+1}} \right. \right. \\
 &\quad \left. \left. + n_3 \{ (v + \delta n_3 - \tau n_4 - \theta n_3n_4) \frac{1}{S^{2\theta+1}} \} \right\} \right] \\
 &= L^{-1} \left[\left\{ v + \delta (b \{ r(1 - bn_3)n_3 - kn_3n_4 \} \frac{t^{2\theta}}{\Gamma(2\theta+1)} \right) \right. \right. \\
 &\quad \left. \left. - \tau \{ v + \delta n_3 - \tau n_4 - \theta n_3n_4 \} \frac{t^{2\theta}}{\Gamma(2\theta+1)} \right. \right. \\
 &\quad \left. \left. - \theta n_4 \{ r(1 - bn_3)n_3 - kn_3n_4 \} \frac{t^{2\theta}}{\Gamma(2\theta+1)} \right. \right. \\
 &\quad \left. \left. + n_3 \{ (v + \delta n_3 - \tau n_4 - \theta n_3n_4) \frac{t^{2\theta}}{\Gamma(2\theta+1)} \} \right\} \right] \quad (24)
 \end{aligned}$$

Similarly, the remaining terms can be derived, ultimately yielding the solution in the form of an infinite series be

$$\begin{aligned}
 S(t) &= S_0 + S_1 + S_{22} + \dots, I(t) = I_0 + I_1 + I_2 + \dots, \\
 C(t) &= C_0 + C_1 + C_2 + \dots, W(t) = W_0 + W_1 + W_2 + \dots, \quad (25)
 \end{aligned}$$

RESULTS AND DISCUSSION

We conduct a numerical simulation to gain deeper insights into the dynamics and control of T cell treatment. With the initial values $S_0 = 149.079, I_0 = 1.082, C_0 = 1.5971, W_0 = 252.26, \theta = \alpha$, and parameters given in Table 1, 2, the simulation's results were evaluated to produce the series solution of arbitrary order that follows.

$$S = 152.079 + \frac{1.75985t^\alpha}{\Gamma(\alpha+1)} - \frac{5.0453249775t^{2\alpha}}{\Gamma(2\alpha+1)}, \quad (26)$$

$$I = 1.082 - \frac{0.039485t^\alpha}{\Gamma(\alpha+1)} - \frac{0.0000294916t^{2\alpha}}{\Gamma(2\alpha+1)}, \quad (27)$$

$$C = 1.5971 - \frac{0.47729t^\alpha}{\Gamma(\alpha+1)} - \frac{.0035676t^{2\alpha}}{\Gamma(2\alpha+1)}, \quad (28)$$

$$W = 252.26 - \frac{15.3218t^\alpha}{\Gamma(\alpha+1)} - \frac{5.705114t^{2\alpha}}{\Gamma(2\alpha+1)}, \quad (29)$$

Numerical Simulation and Comparison of Results

This section will compare the numerical solutions determined using the RK4 method with the analytical solutions of the FO at CAR T cell therapy model for leukemia obtained using the LADM. T-cell parameters $\alpha = 0.001, \beta = 0.00005, \mu = 0.0002$, and $\gamma = 0.001, A = 1.5$, are using serve as the foundation for immune cell characteristics in the ensuing numerical simulations. It is assumed when determining the estimated value of Table 2. Here, Figure 2 illustrates the stability region of the FO system for $0 < \alpha < 1$, as determined by the criterion outlined in Eq. (8.1). Also Figure 3 represents the analytical

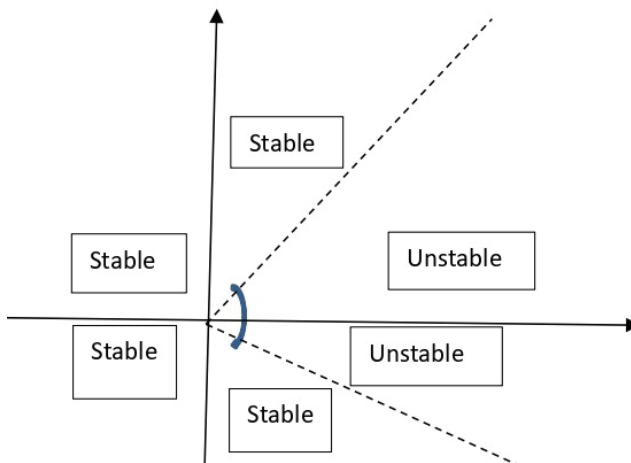


Figure 2. The stability region of the FO system for $0 < \alpha < 1$, as determined by the criterion outlined in Eq. (8.1)

solution for $S(t)$ and approximate solutions obtained using the LADM for various fractional-order values of α within the range $0 < t < 1$. We execute simulation for the static ending time 50 days and plotted Figures 3-11 given below. Using the

LADM, the study computed numerical results for $S(t)$, $I(t)$, $C(t)$, and $W(t)$. We have found that these results are studied in altered values of the FO parameter α . Numerical simulation of $S(t)$, $I(t)$, $C(t)$, and $W(t)$ plotted in Figures 3-11 given below. Over an interval of $0 < t < \alpha$ for various values of $\alpha=1, 0.75, 0.50, 0.25$ respectively and all outcomes have been compared with the analytical solution of the considered problem. Figure 4, $I(t)$ highlight the significance of the effect of each parameter's sensitivity on the important reproduction quantity through two-dimensional plots that show the reactions to two different parameter values. Furthermore, Figure 5, $C(t)$ and, Figure 6, $W(t)$ are represents the analytical solution for approximate solutions obtained using the LADM for various fractional-order values of α within the range $0 < t < 1$ respectively. Here, Figs. 3-6 illustrate that the fractional-order leukemia model offers greater flexibility, allowing for varied responses across different compartments of the proposed model (3). Notably, we assumed relatively small initial values, which justified the use of a short time interval. For extensive time intervals, larger initial values should be considered to ensure that the population values remain positive, and the reverse applies for shorter intervals. Figure 7 represents the plot comparing Susceptible, Infected, Cancer

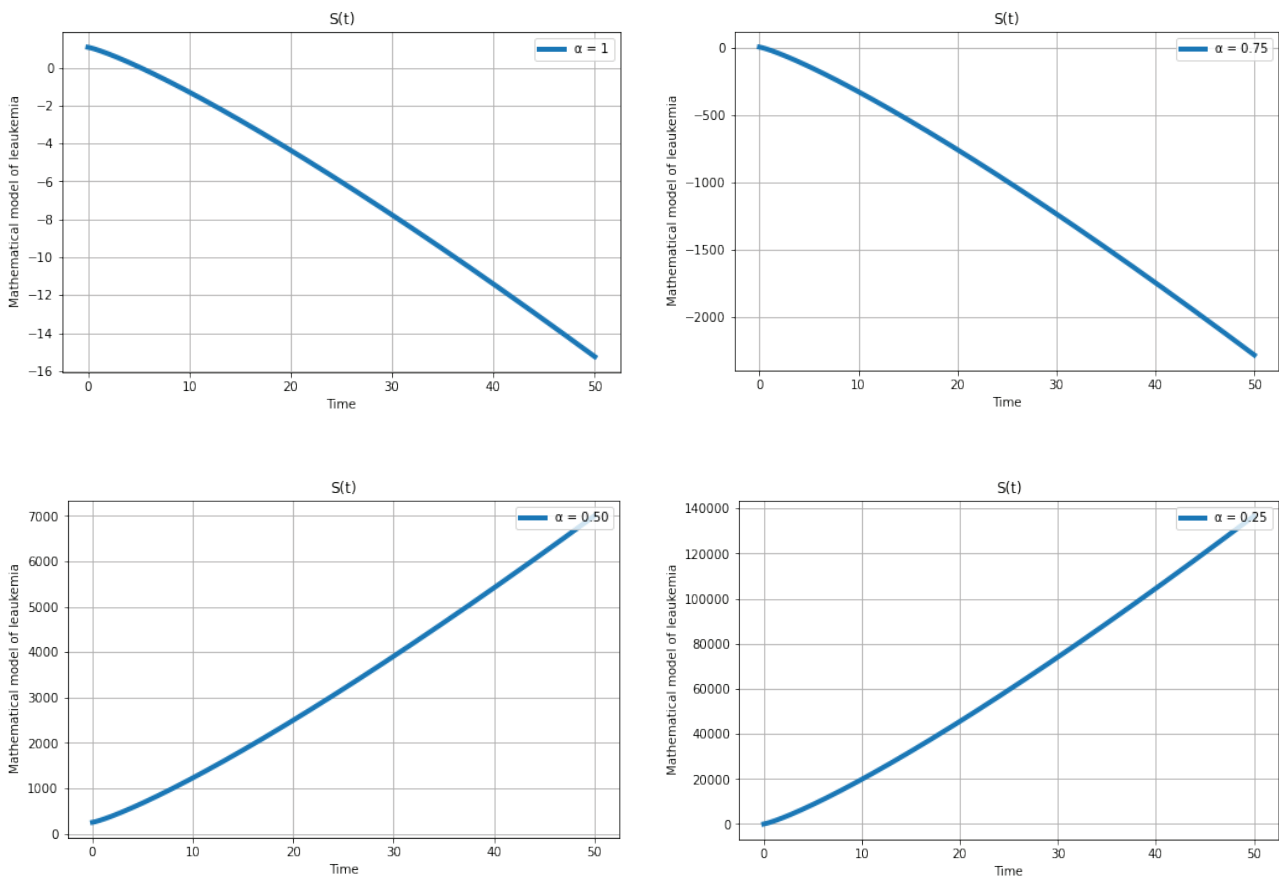


Figure 3. Analytical solution for $S(t)$ and approximate solutions obtained using the LADM for various fractional-order values of α within the range $0 < t < 1$.

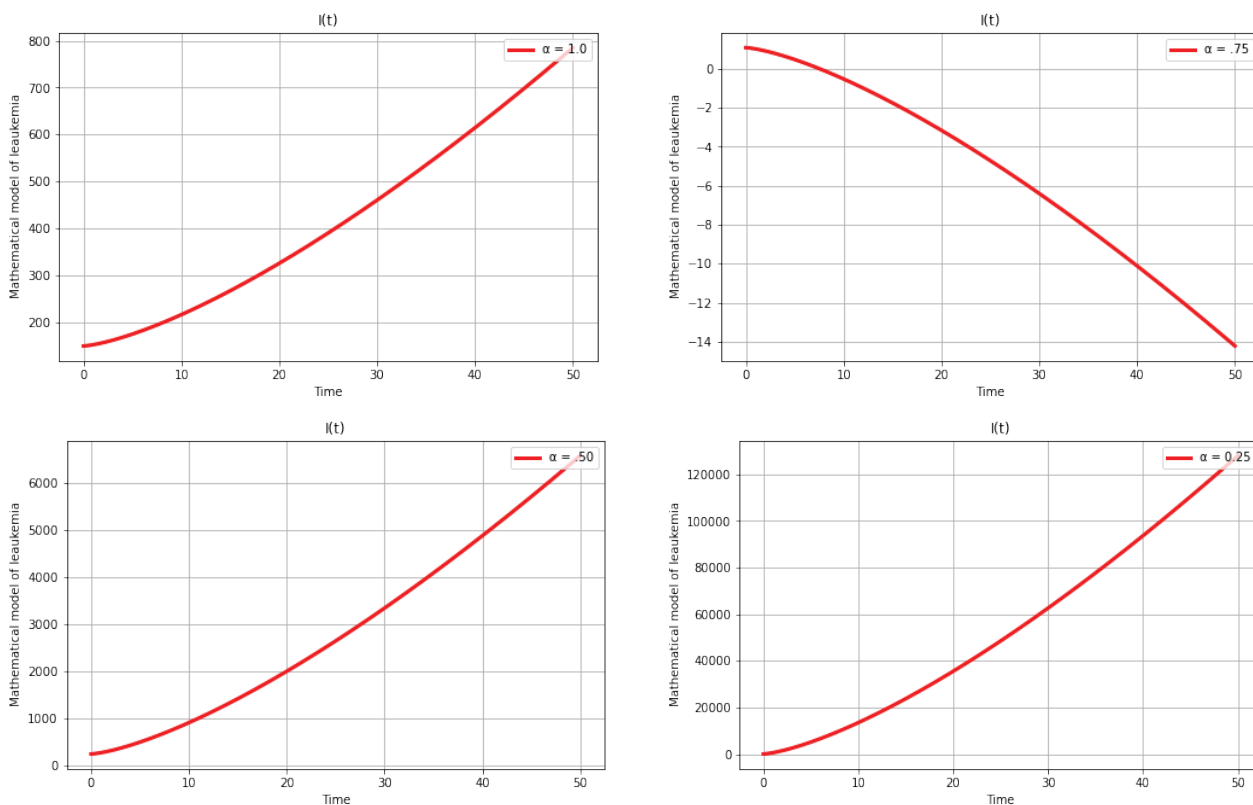


Figure 4. Analytical solution for $I(t)$ and approximate solutions obtained using the LADM for various fractional-order values of α within the range $0 < t < 1$.

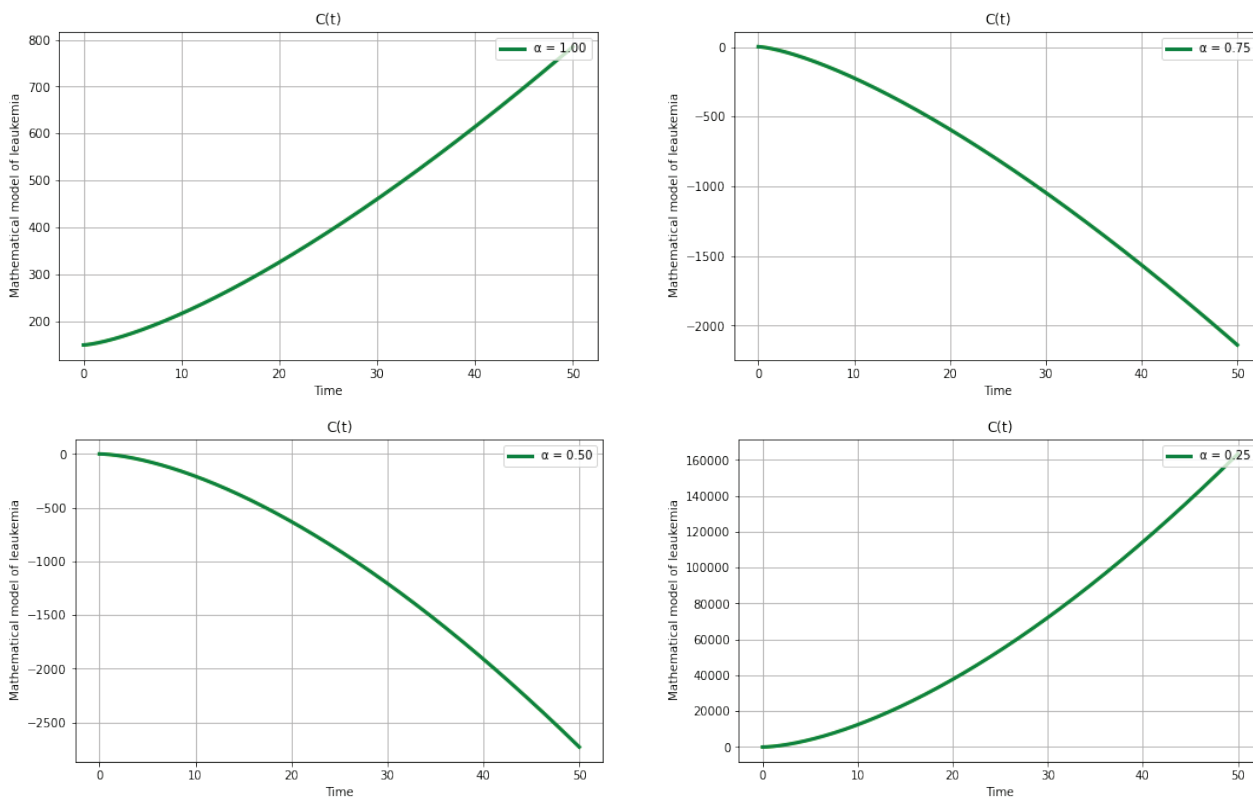


Figure 5. Analytical solution for $C(t)$ and approximate solutions obtained using the LADM for various fractional-order values of α within the range $0 < t < 1$.

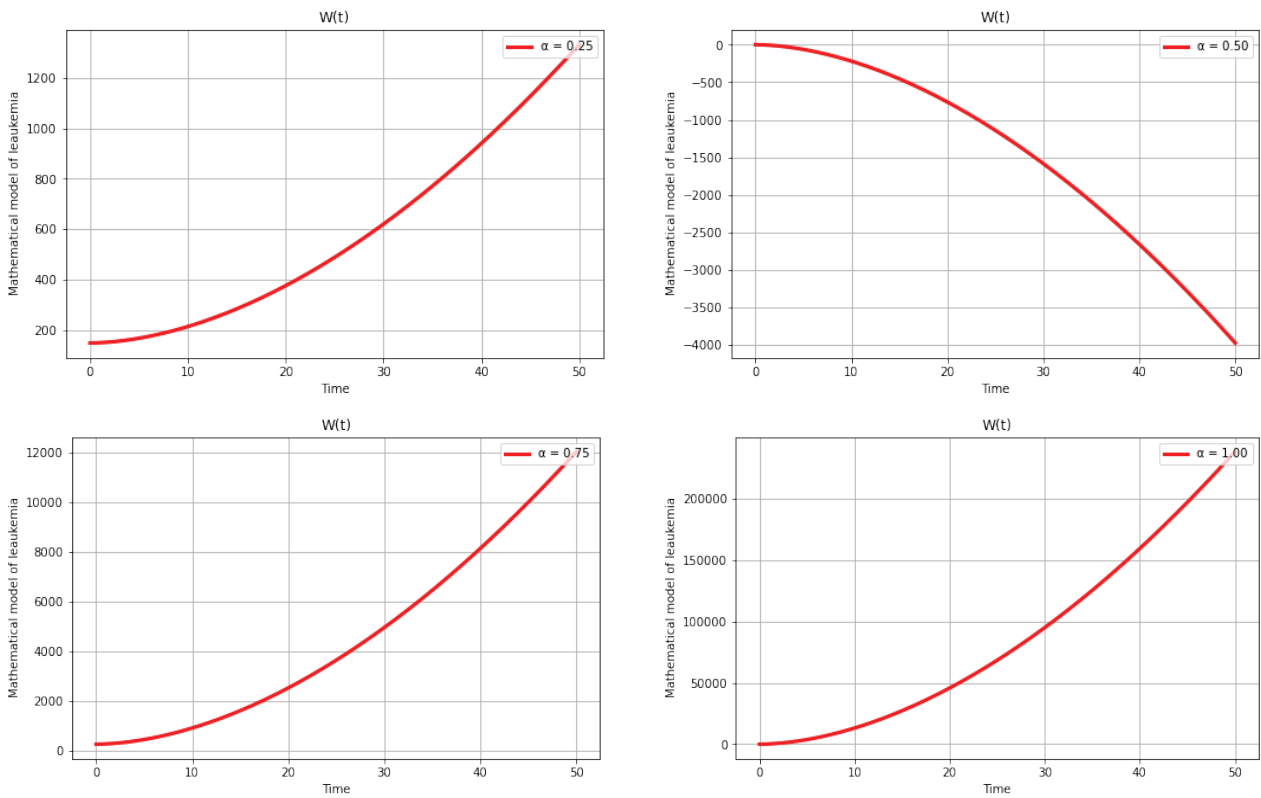


Figure 6. Analytical solution for $W(t)$ and approximate solutions obtained using the LADM for various fractional-order values of α within the range $0 < t < 1$.

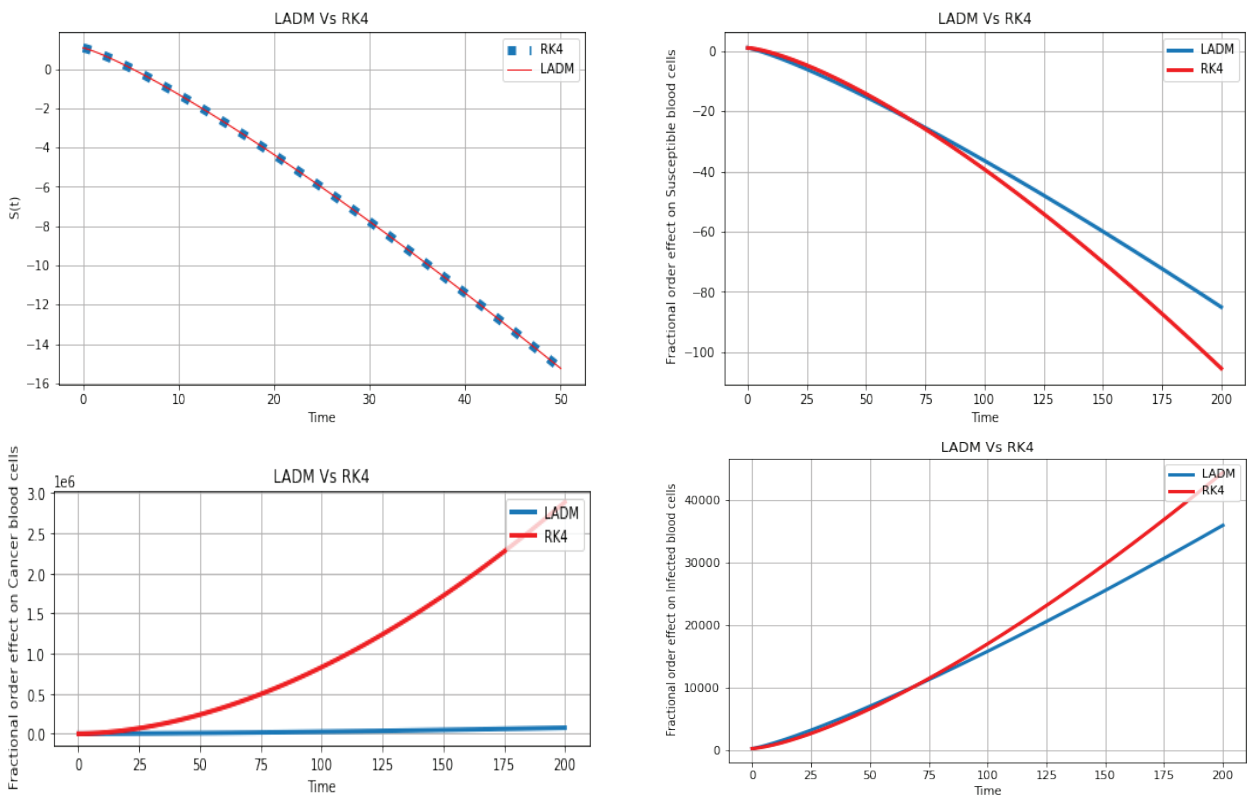


Figure 7. Plot comparing Susceptible, Infected, Cancer and immune blood cells LADM and RK4 method fractional order $\alpha_i = 1$ where $0 < t < 1$.

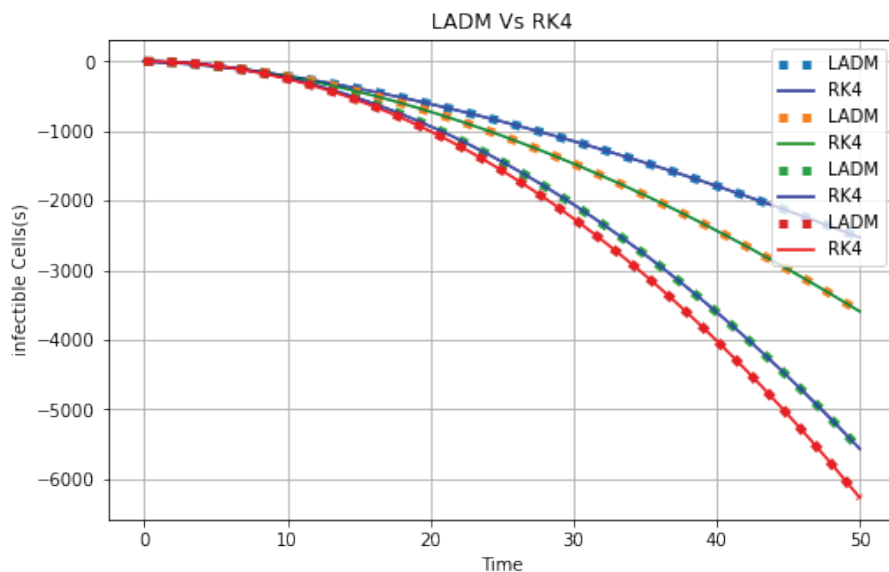


Figure 8. Plot comparing mathematical model of Leukemia LADM and RK4 method FO $\alpha = 1$.

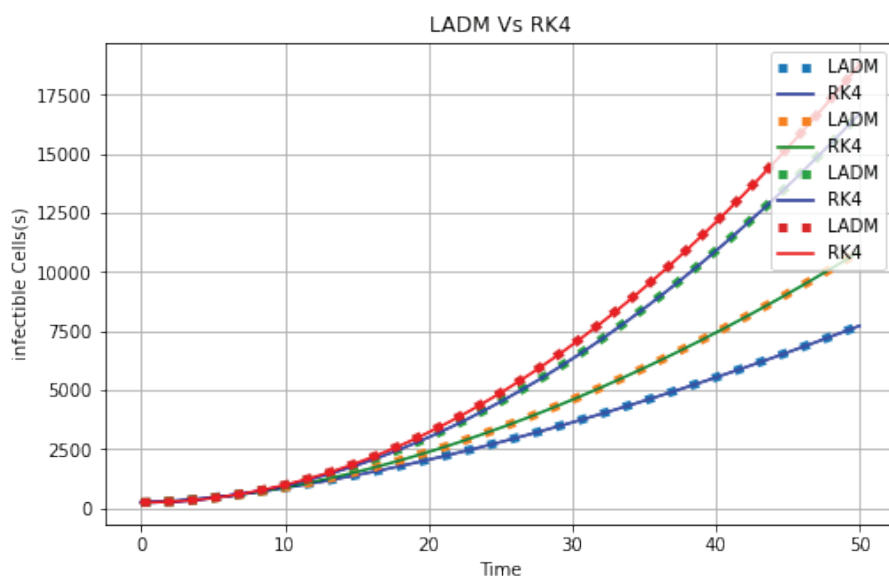


Figure 9. Plot comparing mathematical model of Leukemia LADM and RK4 method FO $\alpha = 0.75$.

and immune blood cells LADM and RK4 method fractional order $\alpha_i = 1$ where $0 < t < 1$ Figure 8-11 present a comparison of the solutions obtained after three terms with those derived using the RK4 method for a classical order α . As shown in Figure 8 - 11 represents the effect of the variation of parameter $\alpha = 1, 0.75, 0.50, 0.25$ respectively on the number $S(t), I(t), C(t),$ and $W(t)$. In this paper, red colors at dotted signed represents RK4 and blue colors represents LADM. We conclude that the analytical solution is much closer to numerical solutions. Hence, our proposed method is reliable and efficient.

Numerical experiments are performed. The results indicate that, for the specified parameter values, the solutions generated by LADM using integer order align closely with those produced by RK4 at the given time. The model of leukemia dynamics within a host are investigated using a fractional-order model that emphasizes adaptive immune memory.

Stability Analysis

The disease-free equilibrium point of the leukemia model (1) is given as

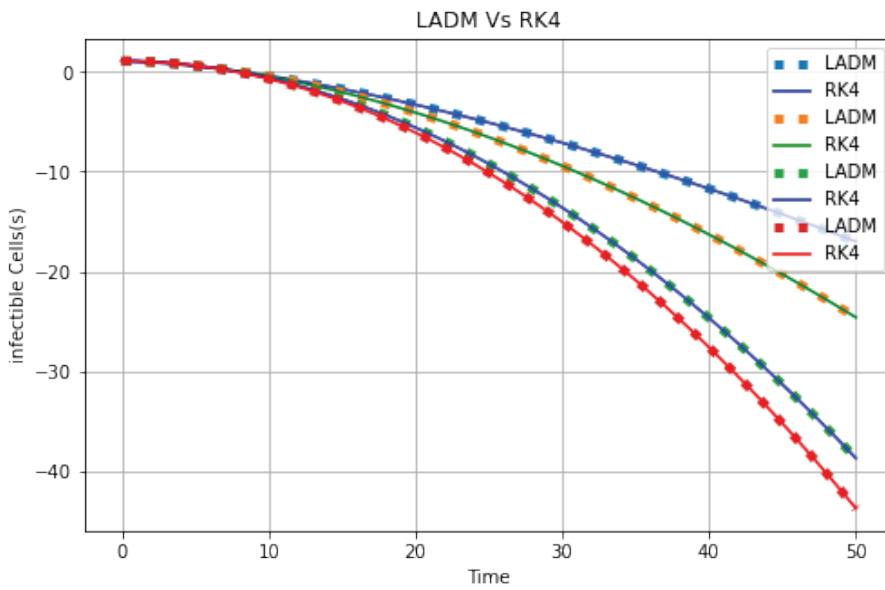


Figure 10. Plot comparing mathematical model of Leukemia LADM and RK4 method FO $\alpha = 0.50$.

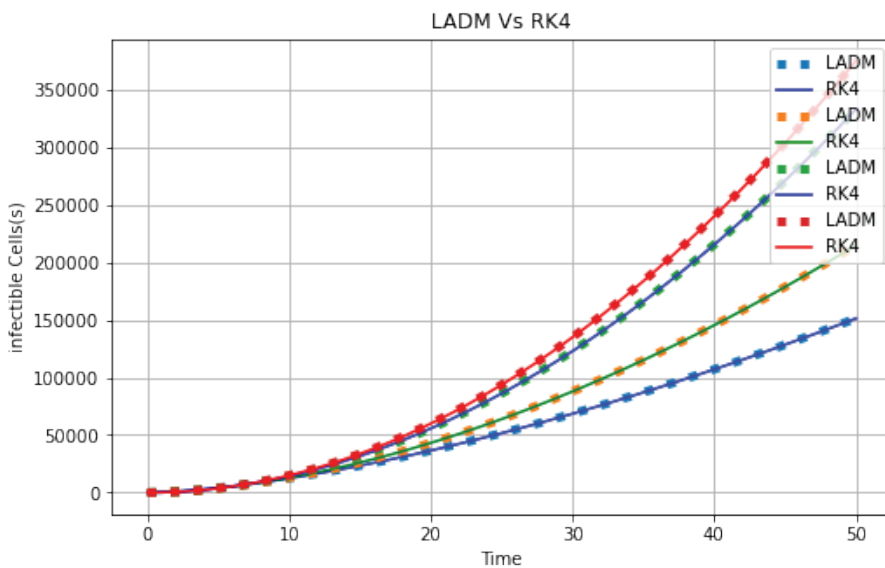


Figure 11. Plot comparing mathematical model of Leukemia LADM and RK4 method FO $\alpha = 0.25$.

$P \equiv (\frac{A}{\alpha}, 0, 0, 0)$ and Endemic equilibrium with the innate immune response point

$$\left(\frac{Abr}{\alpha r b + \beta(r - kC^*)}, \frac{\beta Abr(r - kC^*)}{(\alpha r b + \beta(r - kC^*))(\mu r b + \gamma(r - kC^*))}, \frac{r - kC^*}{r b}, \frac{\delta k + r(\tau b + \theta) \pm \sqrt{\delta k + r(\tau b + \theta)^2 - 2\theta k \delta r}}{2\theta k} \right)$$

Theorem 1: Consider the following autonomous $\frac{d^\alpha v(t)}{dt^\alpha} = g(n(t); n(o)); 0 < \alpha < 1$ nonlinear FO system: The

following systems equilibrium points are solutions to the $g(n(t))=0$. If all eigen values (μ_j) of the jacobian matrix $J = \frac{\partial f}{\partial n}$ meet the condition n^* meet the condition

$$|arg(\mu_j)| > \frac{\alpha \pi}{2}, \tag{30}$$

Then the equilibrium point n^* is locally asymptotically stable.

Proof: Now, let us focus on the asymptotic stability of the endemic (positive) equilibrium for the model described

in (3). To analyze this, we evaluate the Jacobian matrix at the endemic equilibrium, which is expressed as follows:

The J is evaluated at the endemic equilibrium point P^* [4] is given as:

$$J(P^*) = \begin{pmatrix} -\alpha - \beta C^* & 0 & -\beta C^* & 0 \\ \beta C^* & -\mu - \mu C & \beta S^* - \gamma I^* & 0 \\ 0 & 0 & r - 2r\beta C^* - kW^* & -kC^* \\ 0 & 0 & \delta - \theta W^* & -\theta C^* - \tau \end{pmatrix} \quad (31)$$

Now from equation (8.2), we can write as:

$$\mu^4 + l_0\mu^3 + l_1\mu^2 + l_2\mu + l_3 = 0 \quad (32)$$

$$l_0 = V_1 + V_2 + V_3 + V_4 + V_5 + V_6,$$

$$l_1 = V_1V_2 + V_4V_6 + V_1V_4 + V_1V_6 + V_2V_4 + V_2V_6 + V_1V_2V_1^*,$$

$$l_2 = V_1V_4V_6 + V_2V_4V_6 + V_1V_2V_4 + V_1V_2V_6 + V_1V_1pC_1^* + V_1V_2pC_1^*,$$

$$l_3 = V_1V_2V_4V_6 + V_1V_2V_1pC_1^*,$$

$$V_1 = -\alpha_1 - \beta C_1^*, V_2 = \alpha_2 + \beta_1 C_1^*, V_3 = \beta S_1^* - \beta_1 I_1^*,$$

$$V_4 = (2peI_1^* + pW_1^* - p), V_5 = e - b_1W_1^*, V_6 = \alpha_4 + \beta_1 C_1^*.$$

If $V(\varphi)$ denotes the discriminant of polynomial $\varphi(\mu) = \mu^4 + l_0\mu^3 + l_1\mu^2 + l_2\mu + l_3$, where all the coefficients are real.

$$V(\varphi) = \begin{vmatrix} 1 & l_0 & l_1 & l_2 & l_3 & 0 & 0 \\ 0 & 1 & l_0 & l_1 & l_2 & l_3 & 0 \\ 0 & 0 & 1 & l_0 & l_1 & l_2 & l_3 \\ 4 & 3l_0 & 2l_1 & l_2 & 0 & 0 & 0 \\ 0 & 4 & 3l_0 & 2l_1 & l_2 & 0 & 0 \\ 0 & 0 & 4 & 3l_0 & 2l_1 & l_2 & 0 \\ 0 & 0 & 0 & 4 & 3l_0 & 2l_1 & l_2 \end{vmatrix} \quad (33)$$

We have the proposition [44].

Theorem 2. Assume that P^* exists in R^4

I. Proof: Put Ψ_1, Ψ_2, Ψ_3 are Routh-Hourwitz determinants:

$$\Psi_1 = l_0, \Psi_2 = \begin{vmatrix} l_0 & 1 \\ l_2 & l_1 \end{vmatrix}, \Psi_3 = \begin{vmatrix} l_0 & 1 & 0 \\ l_2 & l_1 & l_0 \\ 0 & l_3 & l_2 \end{vmatrix}$$

When $\alpha = 1$, the equilibrium point P^* is locally asymptotically stable if

$$\Psi_1 > 0, \Psi_2 > 0, \Psi_3 = 0, l_3 > 0. \quad (34)$$

For all $\alpha \in [0,1)$, P^* is locally asymptotically stable, these (8.5) be sufficient but no essential. We will investigate the equation (8.1) from $n = 1$ to 4.

II. If $l_3 > 0$ be then point P^* is locally asymptotically stable.

III. If $V(\varphi) > 0, l_0 > 0, l_1 < 0$ and $\alpha > 2/3$ then P^* is equilibrium unstable.

IV. If $V(\varphi) < 0, l_0 < 0, l_1 > 0, l_2 < 0, l_3 > 0$, then P^* is equilibrium unstable.

Convergence Analysis

The obtained solution is a rapidly converging series that consistently approaches the exact solution. To verify the

convergence of the series (15), we employ classical techniques, drawing on the approach outlined in [17].

Theorem 1: Let, R be a Banach space and $N: R \rightarrow R$ be a constructive nonlinear operator such that $\forall r, r^1 \in R, \|N(r) - N(r^1)\| \leq p \|r - r^1\|, 0 < p < 1$. Then N has a unique point m such that $Nr = r$, where $r = (S, I, C, W)$. The series given in (15) can be written by LADM as: $R_y = NR_{y-1}, R_{y-1} = \sum_{i=1}^{y-1} R_i, y = 1, 2, 3, \dots$, and assume that $r_0 \in B_j(r)$ where $B_j(r) = \{r^1 \in R: \|r - r^1\| < j\}$, t then we have

I. $r_y \in B_j(r)$;

II. $\lim_{y \rightarrow \infty} r_y = y$.

Proof: For (I), using mathematical induction for $y = 1$, we have

$$\|r - r^1\| = \|N(r_0) - N(r)\| < p \|r_0 - r\|.$$

Put the result is true for $k - 1$ then

$\|r_0 - r\| \leq p^{k-1} \|r_0 - r\|$. We have

$$\|r_0 - r\| = \|N(r_{k-1}) - N(r)\| \leq p \|r_{k-1} - r\| \leq p^k \|r_0 - r\|.$$

$$\|r_y - r\| \leq p^y \|r_0 - r\| \leq p^y j < j$$

which implies that $r_y \in B_j(r)$.

(II) since $\|r_y - r\| \leq p^y \|r_0 - r\| \leq p^y$ and $\lim_{y \rightarrow \infty} p^y = 0$,

therefore we have $\lim_{y \rightarrow \infty} \|r_y - r\| = 0$ then $\lim_{y \rightarrow \infty} r_y = y$.

Hence the theorem is verified.

CONCLUSION

We have successfully developed a scheme for numerical solutions mathematical model of CAR T-cell therapy of fractional order by using the Adomian decomposition method and the Runge-Kutta fourth order method. The results of the Laplace Adomian decomposition method and the Runge-Kutta fourth order method are compared with each other. Furthermore, the approximate solution by Laplace Adomian decomposition method is in complete agreement with the Runge-Kutta fourth order method for Figs.7-11 respectively. Further, this validates Laplace Adomian decomposition method for efficiency and accuracy in solving the proposed model for leukemia. In these simulations, the study demonstrates the impact on memory on invulnerable dynamics. The dynamic behavior of the structure was visualized as various parameters were varied using the LADM. Finally, this study made a significant insight into the T-cell therapy transmission dynamics. More compartments like as cytokine, vaccination may be added with the Mathematical model of leukemia fractional order differential equation to get more accurate solutions that can be treated as future research of this work.

AUTHOR CONTRIBUTIONS

The main study conception and design provided, Material preparation, Data collection provided by [RK].

Graphical Representation, Result discussion and analysis were performed by [RK], [MAA] and [ABK]. The first draft of the manuscript was written by [ABK], [RK], and [PD]. Conceptualization, research, methodology, supervision, visualization, and writing-review and editing-are all covered by [MAA],[ABK] and [RK].

CONFLICT OF INTEREST

The authors declare that they have no known conflicting financial interests or personal relationships that could have influenced the work disclosed in this publication.

DATA AVAILABILITY STATEMENT

The authors confirm that the data that supports the findings of this study are available within the article. Raw data that support the finding of this study are available from the corresponding author, upon reasonable request.

CONFLICT OF INTEREST

The author declared no potential conflicts of interest with respect to the research, authorship, and/or publication of this article.

ETHICS

There are no ethical issues with the publication of this manuscript.

STATEMENT ON THE USE OF ARTIFICIAL INTELLIGENCE

Artificial intelligence was not used in the preparation of the article.

REFERENCES

- [1] Agarwal M, Bhadauria AS. Mathematical modeling and Analysis of Leukemia: Effect of External Engineered T Cells Infusion. *Appl Applied Math Int J* 2015;10:249–266.
- [2] Altrock PM, Liu LL, Michor F. The mathematics of cancer: Integrating quantitative models. *Nature* 2015;15:730–745. [\[CrossRef\]](#)
- [3] Mutlu B, Ozyoruk B. A research on mathematical model approaches in biomass supply chain. *Sigma J Eng Nat Sci* 2024;42:945–955. [\[CrossRef\]](#)
- [4] Khumaeroh MS, Shalehah MA, Ilahi F. Mathematical model of Leukemia Treatment with Chimeric Antigen Receptor (CAR) T Cell Therapy. *Mathline* 2023;8:1077–1090. [\[CrossRef\]](#)
- [5] Elsayad K, Oertel M, Haverkamp U, Eich HT. The effectiveness of radiotherapy for leukemia cutis. *J Cancer Res Clin Oncol* 2017;143:851–859. [\[CrossRef\]](#)
- [6] Manoj P, Punith KB, Manjunath KC. Enhancing road safety through blackspots mitigative measures-A review. *Sigma J Eng Nat Sci* 2024;42:1670–1682. [\[CrossRef\]](#)
- [7] June CH, O'Connor RS, Kawalekar OU, Ghassemi S, Milone MC. CAR T cell immunotherapy for human cancer. *Science* 2018; 359:1361–1365. [\[CrossRef\]](#)
- [8] Khatun MS, Biswas MHA. Modeling the effect of adoptive T cell therapy for the treatment of leukemia. *Comput Math Meth* 2020;2:1–16. [\[CrossRef\]](#)
- [9] Akdas E, Eren T. A sample application for scheduling search and rescue teams in an earthquake disaster. *Sigma J Eng Nat Sci* 2024;42:1555–1562. [\[CrossRef\]](#)
- [10] Lee DW, Gardner R, Porter DL, Louis CU, Ahmed N, Jensen M, et al. Current concepts in the diagnosis and management of cytokine release syndrome. *Blood* 2014;124:188–195. [\[CrossRef\]](#)
- [11] Gunerhan H, Kaabar MKA, Celik E. Novel analytical and approximate-analytical methods for solving the nonlinear fractional smoking mathematical model. *Sigma J Eng Nat Sci* 2023;41:331–343. [ABK], [RK],
- [12] Gogoi UN, Saikia P, Mahanta DJ. Rapid parameter estimation of four non-linear growth models for analyzing the growth of *Escherichia Coli*. *Sigma J Eng Nat Sci* 2024;42:778–786. [\[CrossRef\]](#)
- [13] Olayiwola MO, Alaje AI, Olarewaju AY, Adedokun KA. A caputo fractional order epidemic model for evaluating the effectiveness of high-risk quarantine and vaccination strategies on the spread of COVID-19. *Healthc Anal* 2023;3:100179. [\[CrossRef\]](#)
- [14] Alaje AI, Olayiwola MO, Adedokun KA, Adedeji JA, Oladapo AO, Akeem YO. The modified homotopy perturbation method and its application to the dynamics of price evolution in Caputo-FO Black Scholes model. *Beni-Suef Univ J Basic Appl Sci* 2023;12:93. [\[CrossRef\]](#)
- [15] Olayiwola MO, Alaje AI, Yunus AO. A caputo fractional order financial mathematical model analyzing the impact of an adaptive minimum interest rate and maximum investment demand. *Results Control Optim* 2023;100349. [\[CrossRef\]](#)
- [16] Alaje IA, Olayiwola MO. A Fractional order MM for examining the spatiotemporal spread of COVID-19 in the presence of vaccine distribution. *Healthc Anal* 2023;4:100230. [\[CrossRef\]](#)
- [17] Haq F, Shah K, Rahman G, Shahzad M. Numerical solution of fractional order smoking model via Laplace Adomian decomposition method. *Alex Eng J* 2018;57:1061–1069. [\[CrossRef\]](#)
- [18] Yunus AO, Olayiwola MO, Adedokun KA, Adedeji JA, Alaje IA. Mathematical analysis of fractional-order Caputo's derivative of coronavirus disease model via Laplace Adomian decomposition method. *Beni-Suef Univ J Basic Appl Sci* 2022;11:144. [\[CrossRef\]](#)

- [19] Dehingia K, Mohsen AA, Alharbi SA, Alsemiry RD, Rezapour S. Dynamical behavior of a FO model for withinhost SARS-CoV-2. *Mathematics* 2022;10:2344. [\[CrossRef\]](#)
- [20] Cancer Today. Available at: <https://gco.iarc.fr/today/home>. Accessed on 17 Mar 2026.
- [21] Arqub OA, Maayah B. Adaptive the Dirichlet model of mobile/immobile advection/dispersion in a time-fractional sense with the reproducing kernel computational approach: Formulations and approximations. *Int J Mod Phys B* 2023;37:2350179. [\[CrossRef\]](#)
- [22] Maayah B, Arqub OA. Hilbert approximate solutions and fractional geometric behaviors of a dynamical fractional model of social media addiction affirmed by the fractional Caputo differential operator. *Chaos, Solitons, Fract: X* 2023;10:100092. [\[CrossRef\]](#)
- [23] Maayah B, Arqub OA, Alnabulsi S, Alsulami H. Numerical solutions and geometric attractors of a fractional model of the cancer-immune based on the Atangana-Baleanu-Caputo derivative and the reproducing kernel scheme. *Chin J Phys* 2022;80:463–483. [\[CrossRef\]](#)
- [24] Nuraini N, Tasman H, Soewono E, Sidarto KA. A with-in host dengue infection model with immune response. *Math Comput Model* 2009;49:1148–1155. [\[CrossRef\]](#)
- [25] Yao SW, Arqub OA, Tayebi S, Osman MS, Mahmoud W, Inc M, et al. A novel collective algorithm using cubic uniform spline and finite difference approaches to solving fractional diffusion singular wave model through damping-reaction forces. *Fractals* 2023;31:2340069. [\[CrossRef\]](#)
- [26] Shah K, Jarad F, Abdeljawad T, On a nonlinear FO model of dengue fever disease under Caputo-Fabrizio derivative. *Alex Eng J* 2020;59:2305–2313. [\[CrossRef\]](#)
- [27] Borah M, Gayan A, Sharma JS, Chen Y, Wei Z, Pham VT. Is fractional-order chaos theory the new tool to model chaotic pandemics as COVID-19?. *Nonlinear Dynam* 2022;109:1187–1215. [\[CrossRef\]](#)
- [28] Das K, Kumar GR, Ramesh K, Biswas HA. A Qualitative Analysis of Leukemia Fractional Order SICW Model. *Jambura J Biomath* 2024;5:46–53. [\[CrossRef\]](#)
- [29] Ponalagusamy R, Murugesan K, Dhayabaran DP, Amirtharaj ECH. Numerical solution of heat flow problem by a combined method of rayleigh ritz with STWS and RKHM. *Adv Model Anal A* 2001;38:29–48.
- [30] Ponalagusamy R. A Novel and Efficient Computational Algorithm of STWS for Generalized Linear Non-Singular/Singular Time Varying Systems. *J Softw Eng* 2008;2:1–9. [\[CrossRef\]](#)
- [31] Ponalagusamy R, Senthilkumar S. A comparison of rk-fourth orders of variety of means and embedded means on multilayer raster CNN simulation. *J Theor Appl Inf Technol* 2007; 3.
- [32] Ponalagusamy R, Alphonse PJA, Chandru M. Development of new fifth-order fifth-stage Runge Kutta method based on heronian mean. *Int J Eng Sci* 2011;2:162–197.
- [33] Chandru M, Ponalagusamy R, Alphonse PJA. A New Fifth-Order Weighted Runge-Kutta Algorithm Based on Heronian Mean for Initial Value Problems in Ordinary Differential Equations. *J Appl Math Inf* 2017;35:191–204. [\[CrossRef\]](#)
- [34] Ponalagusamy R, Senthilkumar S. A new fourth order embedded RKAHeM (4, 4) method with error control on single layer/raster cellular neural network. *Springer* 2009;3:303–305. [\[CrossRef\]](#)
- [35] Atalan A, Donmez NFK, Donmez CC. Developing optimization models to evaluate healthcare systems. *Sigma J Eng Nat Sci* 2020;38:853–873.
- [36] Karim, R., Akbar, M. A., Pk, M. B., & Dey, P. A study on fractional-order mathematical and parameter analysis for CAR T-cell therapy for leukemia using homotopy perturbation method. *Partial Differential Equations in Applied Mathematics* 2025; 14: 101152.
- [37] Ozgur B, Demir A. The stability analysis of a neural field model with small delay. *Sigma J Eng Nat Sci* 2024;42:900–904. [\[CrossRef\]](#)
- [38] Karim R, Bkar pk MA, Dey P, Akbar MA, Osman MS. A study about the prediction of population growth and demographic transition in Bangladesh. *J Umm Al-Qura Univ Appl Sci* 2024;11:91–103. [\[CrossRef\]](#)
- [39] Maude SL, Laetsch TW, Buechner J, Rives S, Boyer M, Bader P, et al. Tisagenlecleucel in Children and Young Adults with B-Cell Lymphoblastic Leukemia. *N Engl J Med* 2018;378:439–448. [\[CrossRef\]](#)
- [40] Liao SJ. An approximate solution technique not depending on small parameters: a special example. *Int J Non-Linear Mech* 1995;30:371–380. [\[CrossRef\]](#)
- [41] He JH. Homotopy perturbation technique. *Comput Methods Appl Mech Eng* 1999;178:257–262. [\[CrossRef\]](#)
- [42] Ahmed E, El-Sayed AMA, El-Saka HA. On some Routh–Hurwitz conditions for fractional order differential equations and their applications in Lorenz, Rössler, Chua and Chen systems. *Phys Lett A* 2006;358:1–4. [\[CrossRef\]](#)
- [43] Raghu A, Gajjela N, Garvandha M. MHD Maxwell dusty fluid in thermally stratified radiative flow with temperature-dependent thermal conductivity and Cattaneo-Christov model. *Heliyon* 2024;10:e30355. [\[CrossRef\]](#)
- [44] Raghu A, Gajjela N, Aruna J, Niranjana H. Significance of modified Fourier heat flux on Maxwell hybrid (Cu-Al₂O₃/H₂O) nanofluid transport past an inclined stretching cylinder. *J Therm Anal Calorim* 2024;1–19. [\[CrossRef\]](#)
- [45] Garvandha M, Gajjela N, Narla V, Kumar D. Thermodynamic entropy of a magnetized nanofluid flow over an inclined stretching cylindrical surface. *J Therm Eng* 2021;10:1253–1265. [\[CrossRef\]](#)